

# Optimization of $\text{Al}_2\text{O}_3/\text{SiN}_x$ stacked antireflection structures for N-type surface-passivated crystalline silicon solar cells\*

Wu Dawei(吴大卫)<sup>†</sup>, Jia Rui(贾锐), Ding Wuchang(丁武昌), Chen Chen(陈晨), Wu Deqi(武德起), Chen Wei(陈伟), Li Haofeng(李昊峰), Yue Huihui(岳会会), and Liu Xinyu(刘新宇)

Institute of Microelectronics, Chinese Academy of Sciences, Beijing 100029, China

**Abstract:** In the case of N-type solar cells, the anti-reflection property, as one of the important factors to further improve the energy-conversion efficiency, has been optimized using a stacked  $\text{Al}_2\text{O}_3/\text{SiN}_x$  layer. The effect of  $\text{SiN}_x$  layer thickness on the surface reflection property was systematically studied in terms of both experimental and theoretical measurement. In the stacked  $\text{Al}_2\text{O}_3/\text{SiN}_x$  layers, results demonstrated that the surface reflection property can be effectively optimized by adding a  $\text{SiN}_x$  layer, leading to the improvement in the final photovoltaic characteristic of the N-type solar cells.

**Key words:** antireflection coatings; aluminum oxide; silicon nitride; simulation; solar cells

**DOI:** 10.1088/1674-4926/32/9/094008

**EEACC:** 2520

## 1. Introduction

The N-type based solar cell, as one of the promising alternatives to conventional solar cells, has attracted extensive research attention due to its several advantages. Compared with p-type silicon, n-type silicon is more tolerant to common metal contaminations<sup>[1]</sup>. Also, n-type silicon shows no light-induced degradation, which is known as a defect for p-type CZ silicon due to boron–oxygen pairs<sup>[2]</sup>. With conversion efficiencies above 23%, the potential of n-type silicon has been demonstrated at the device level in recent years<sup>[3,4]</sup>.

In the case of N-type based solar cells, a boron diffused (p-type) emitter was commonly formed as the pn junction. In such a solar cell structure, the antireflection coating as well as the surface passivation is of crucial importance to optimize the final photovoltaic performance of a p-type emitter. However, common dielectric layers for the passivation of an n+ emitter, for example  $\text{SiN}_x$ ,  $\text{SiO}_2$ , do not show the same performance as the p+ emitter<sup>[5]</sup>. Thin films of aluminum oxide ( $\text{Al}_2\text{O}_3$ ) grown by atomic layer deposition (ALD) are known to provide an excellent level of surface passivation on lowly<sup>[6]</sup> and highly<sup>[7]</sup> boron-doped p+ surfaces. Although the single  $\text{Al}_2\text{O}_3$  layer can passivate the p-type emitter, the growth of such a layer suffers from the slow growth rate using the ALD process, and the anti-reflection property is not satisfactory. Hence, an extra antireflection coating (ARC) layer, e.g.  $\text{SiN}_x$ , has to be added to form the stacked surface passivation.

The surface passivation property of an  $\text{Al}_2\text{O}_3/\text{SiN}_x$  stacked layer has been studied systematically thus far<sup>[8]</sup>. Nevertheless, for the  $\text{Al}_2\text{O}_3/\text{SiN}_x$  stacked layer, the effect of  $\text{SiN}_x$  thickness on the surface anti-reflection property is still in its infancy. In this paper, we report the optimized  $\text{SiN}_x$  thickness value, and verify the simulation results in experiments based

on the theoretical computational simulation analysis. The effect of emitter passivation and the theoretical highest efficiency of p+nn+ type solar cells extracted from Afors-Het simulation were also studied.

## 2. Theory

The optical matrix approach is usually employed for calculation of the reflection coefficient. The main idea of this method matches the E- and H-fields of the incident light on the interfaces of the two layer optical coatings. The matrix relation defining the two layer antireflection coating problem is given in Ref. [9],

$$\begin{bmatrix} B \\ C \end{bmatrix} = \left\{ \prod_{r=1}^q \begin{bmatrix} \cos \delta_r & (i \sin \delta_r)/\eta_r \\ i\eta_r \sin \delta_r & \cos \delta_r \end{bmatrix} \right\} \begin{bmatrix} 1 \\ \eta_m \end{bmatrix}, \quad (1)$$

where  $\delta_r = (2\pi N d \cos \theta_r)/\lambda$  and  $\eta_m$  is substrate admittance. The tilted optical admittance  $\eta$  is given by

$$\eta_p = \frac{N_y}{\cos \theta}, \quad \text{p-waves}, \quad (2)$$

$$\eta_s = N_y \cos \theta, \quad \text{s-waves}. \quad (3)$$

$B$  and  $C$  are total electric and magnetic field amplitudes of the light propagating in the medium. Thus the optical admittance is given by the ratio

$$Y = \frac{C}{B}. \quad (4)$$

The following relations give reflectance, transmittance and absorbance, respectively.

\* Project supported by the State Key Development Program for Basic Research of China (Nos. 2006CB604904, 2009CB939703), the National Natural Science Foundation of China (Nos. 60706023, 60676001, 90401002, 90607022), the Chinese Academy of Sciences (No. YZ0635), and the Chinese Academy of Solar Energy Action Plan.

<sup>†</sup> Corresponding author. Email: wudawei@ime.ac.cn

Received 2 April 2011, revised manuscript received 28 April 2011

© 2011 Chinese Institute of Electronics

$$R = \left( \frac{\eta_0 - Y}{\eta_0 + Y} \right) \left( \frac{\eta_0 - Y}{\eta_0 + Y} \right)^* \quad (5)$$

$$T = \frac{4\eta_0 \text{Re}(\eta_m)}{(\eta_0 B + C)(\eta_0 B + C)^*} \quad (6)$$

$$A = 1 - T - R = (1 - R) \left( 1 - \frac{\text{Re}(\eta_m)}{\text{Re}(BC^*)} \right) \quad (7)$$

Thus, each layer is represented by a  $2 \times 2$  matrix  $M$ , of the form

$$M_r = \begin{bmatrix} \cos \delta_r & (i \sin \delta_r) / \eta_r \\ i \eta_r \sin \delta_r & \cos \delta_r \end{bmatrix} \quad (8)$$

For solar cells, it is important to have a minimum reflection over the entire visible spectrum (300–1100 nm). The cell performance is influenced by other parameters, such as the photon flux  $F(\lambda)$ . Since the reflection coefficient needs to be minimized where  $F(\lambda)$  have their maximum values, the weighted reflectance  $R_w$  is calculated from Ref. [10],

$$R_w = \frac{\int_{\lambda_2}^{\lambda_1} F_i(\lambda) R(\lambda) d\lambda}{\int_{\lambda_2}^{\lambda_1} F_i(\lambda) d\lambda} \quad (9)$$

The  $F(\lambda)$  value is extracted according to the AM 1.5 solar spectrum, and  $\lambda_1 = 300$  nm,  $\lambda_2 = 1100$  nm.

### 3. Experiments

In experiment, a 300- $\mu$ m thick boron-doped p-type (100) FZ-Si wafer with a resistivity of 3.5  $\Omega$ -cm was used, in which both sides were polished and used to eliminate the effects of surface roughness. All wafers were thoroughly cleaned using 5% diluted hydrofluoric acid to remove native oxide. The  $\text{Al}_2\text{O}_3$  films were deposited by thermal ALD in an Beneq TSF200 reactor at a substrate temperature of 200  $^\circ\text{C}$ . The cycle times were  $\sim 5$  s and the growth-per-cycle was 1.0 s. The cycles were repeated until the target film thickness 10 nm was finished. Then the  $\text{SiN}_x$  layers with different layer thicknesses were deposited by an Unaxis Plasma Therm790+ PECVD system at a substrate temperature of 350  $^\circ\text{C}$ . The flow rates of silane and ammonia gases to deposit  $\text{SiN}_x$  films were 8.5 and 200 sccm, respectively. The thicknesses of  $\text{SiN}_x$  were changed from 35 nm to 95 nm, with a deviation of 15 nm. The deposition rate of  $\text{SiN}_x$  films was 30 nm/min. The refractive indexes of  $\text{Al}_2\text{O}_3$  and  $\text{SiN}_x$  were measured to be 1.64 and 1.96 using spectroscopic ellipsometry, respectively. The reflectance of wafers coated with  $\text{Al}_2\text{O}_3/\text{SiN}_x$  stacked layers was measured for comparison. The reflectance was characterized at room temperature by a measurement system using a xenon lamp as a light source.

As shown in Fig. 1, the surface reflection spectra of the single  $\text{Al}_2\text{O}_3$  and  $\text{SiN}_x$  layers was demonstrated for a p-type emitter via a Matlab simulation. The theory utilized in this simulation is elaborated in the theory section. In the simulation, given by Ref. [11], the refractive index of  $\text{Al}_2\text{O}_3$  and  $\text{SiN}_x$  is adopted as 1.64 and 1.96 at 2.0 eV, respectively. To achieve the lowest surface reflectance index, the simulation process verified that the optimized thickness of the  $\text{Al}_2\text{O}_3$  single layer and

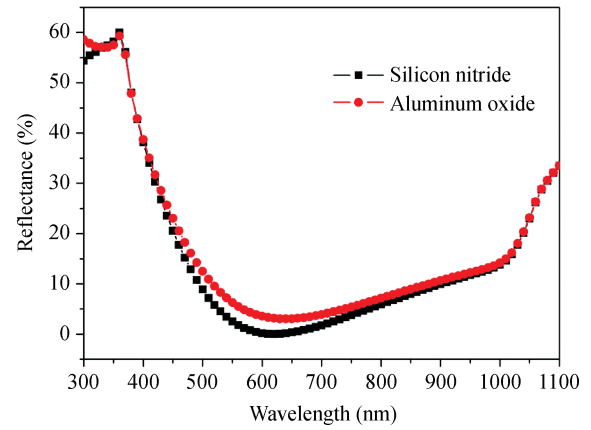


Fig. 1. Surface reflection spectra of the optimized  $\text{Al}_2\text{O}_3$  single layer (square line), and the reflection spectra of the optimized  $\text{SiN}_x$  single layer for a p-type emitter via a Matlab simulation.

the  $\text{SiN}_x$  single layer is determined to be 95 nm and 75 nm, respectively. As shown in Fig. 1, the reflectance of the  $\text{SiN}_x$  single layer seems to be slightly lower than that of the  $\text{Al}_2\text{O}_3$  layer within the whole wavelength range from 300 nm to 1100 nm. The weighted reflectance of the  $\text{SiN}_x$  and  $\text{Al}_2\text{O}_3$  layers is 12.27% and 10.52%, respectively. Compared with the reflectance value of the  $\text{SiN}_x$  layer, the deviation was increased to this maximum around the wavelength of 600 nm (the highest density of photon flux) within the incident sunlight spectra, resulting in the lower weighted reflectance value of the single  $\text{Al}_2\text{O}_3$  layer.

As shown in Fig. 1, the reflection spectra result shows that within the whole incident spectra, the reflectance value of the  $\text{Al}_2\text{O}_3$  single layer seems to be higher than that of the  $\text{SiN}_x$  single layer, leading to a higher weighted reflectance value. It could be inferred that only using the  $\text{Al}_2\text{O}_3$  single layer can passivate the p-type emitter surface. However, the anti-reflection property is not optimized. Taking account of the anti-reflection property as well as the surface passivation, the  $\text{SiN}_x$  layer has to be added to form the stacked  $\text{Al}_2\text{O}_3/\text{SiN}_x$  layers in order to achieve a better anti-reflection property for a p-type emitter. Furthermore, as the  $\text{SiN}_x$  anti-reflection layer can be grown by the PECVD process with a high yielding rate, the incorporation of the  $\text{SiN}_x$  layer enables the shortened yielding process for the stacked  $\text{Al}_2\text{O}_3/\text{SiN}_x$  layers. And, the thermal stability of the ultrathin  $\text{Al}_2\text{O}_3$  is significantly improved by depositing a capping layer of  $\text{SiN}_x$  onto the  $\text{Al}_2\text{O}_3$ , which is probably due to the very high (10–15 at.%) hydrogen content in the PECVD-deposited  $\text{SiN}_x$  film. Therefore, it is worthwhile further analyzing the property of the stacked  $\text{Al}_2\text{O}_3/\text{SiN}_x$  layers as an effective anti-reflection coating for a p-type emitter.

In Fig. 2, we examined the anti-reflection property of the stacked  $\text{Al}_2\text{O}_3/\text{SiN}_x$  layers with different  $\text{SiN}_x$  layers thicknesses by fixing the  $\text{Al}_2\text{O}_3$  layer thickness as 10 nm. As shown in Fig. 2, with an increase in the  $\text{SiN}_x$  layer thickness from 35 to 95 nm, the weighted reflectance of the stacked  $\text{Al}_2\text{O}_3/\text{SiN}_x$  layers was first decreased and then increased. The best result with the lowest weighted reflectance appears at the thickness of 65 nm of  $\text{SiN}_x$  capping layer, with a weighted reflectance of 10.50%. And the reflectance of the 65 nm  $\text{SiN}_x$  capping layer is 9.39% in experimental measurement. This dependence of the

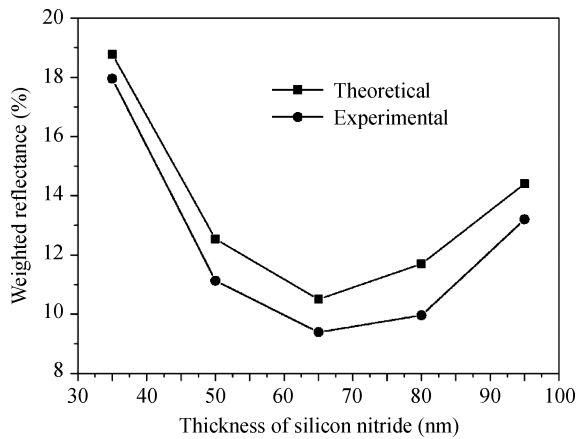


Fig. 2. Theoretical and experimental results of the weighted reflectance as a function of thickness of silicon nitride in an  $\text{Al}_2\text{O}_3/\text{SiN}_x$  stacked layers.

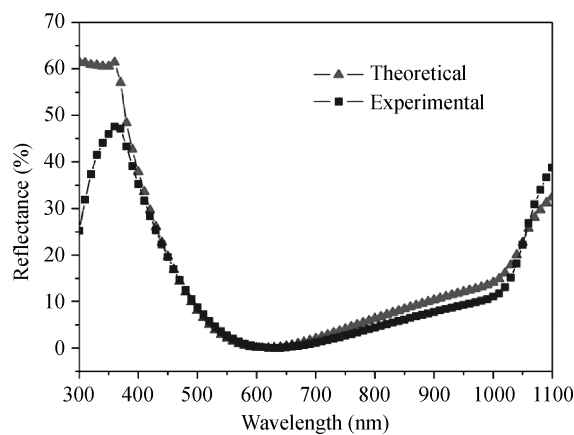


Fig. 3. Optimized surface reflection property using the stacked  $\text{Al}_2\text{O}_3/\text{SiN}_x$  layers both experimentally and theoretically.

thickness in the stacked  $\text{Al}_2\text{O}_3/\text{SiN}_x$  layers can be explained by the weighted reflectance theory. When the thickness of the  $\text{SiN}_x$  layer increased from 35 to 65 nm, the minimum value of the reflectance spectra shifted within the weighted region, resulting in a decrease in the weighted reflectance value. On the other hand, when the thickness of the layer further increased above 65 nm, the minimum value shifted out of the weighted region, leading to an increase in the weighted reflectance. The measured curve, as shown in Fig. 2, shows very good agreement between the theoretical and experimental results. The difference between the two main attributes to the refractive index of the silicon substrate used in the simulation. And the refractive index of  $\text{Al}_2\text{O}_3$  may be increasing for the higher temperature during the deposition process of  $\text{SiN}_x$ , and also the surface coverage would be improved by the increase in thickness of  $\text{SiN}_x$  layer.

Figure 3 shows the optimized surface reflection property using the stacked  $\text{Al}_2\text{O}_3/\text{SiN}_x$  layers both experimentally and theoretically. The two curves fit well within an interesting wavelength region. The difference between the two curves within the short-wavelength response was mainly due to the different refractive indexes of silicon substrate used in simulation and in experiment. The intensity of the xenon lamp used

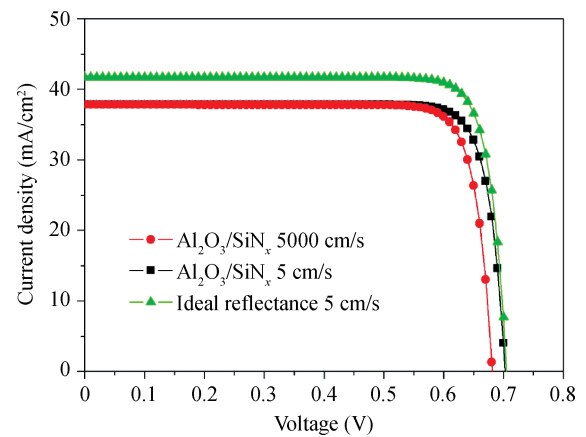


Fig. 4.  $C-V$  curves of the different antireflection and passivation controlled solar cells under standard test conditions (AM 1.5 irradiation,  $T = 300\text{ K}$  and  $P = 100\text{ mW/cm}^2$ ).

in the measurement system was not strong in such a spectrum region. In the long wavelength region from 700 to 1050 nm, the incident light could be reflected by the rear surface of the  $\text{Al}_2\text{O}_3/\text{SiN}_x$  layers, and then collected by the CCD. However, this portion of reflected light was not taken into consideration during the simulation process, which is attributed to the deviation between the simulation and experimental results. We added a simple interface reflection film and achieved a more consistent result.

Next we used Afor-Het software to study the effect of the antireflection and passivation property on a p+nn+ silicon solar cell. Figure 4 plots the current-voltage ( $C-V$ ) curves of the different antireflection and passivation controlled solar cells under standard test conditions (AM 1.5 irradiation,  $T = 300\text{ K}$  and  $P = 100\text{ mW/cm}^2$ ). As shown in Fig. 4, compared to the cell using the same antireflection data from the previous simulation with a higher SRV (surface recombination velocity) of 5000 cm/s, the cell with a SRV of 5 cm/s cell exhibits a 3.2% increase in  $V_{oc}$  due to the better passivation. With a fixed SRV of 5 cm/s, the ideal reflectance (i.e. surface reflectance equals 0) cell exhibits a 10.14% higher  $J_{sc}$  than the cell using the previous reflection data. And the ideal cell presented here can get a high efficiency of 24.85%. We can infer that the antireflection is more important than passivation in a p+nn+ solar cell. Through other methods like texturing, a better solar cell performance can be expected.

#### 4. Conclusion

The anti-reflection property of N-type solar cells has been optimized using a stacked  $\text{Al}_2\text{O}_3/\text{SiN}_x$  layer consisting of 10 nm  $\text{Al}_2\text{O}_3$  and 65 nm  $\text{SiN}_x$ . This further improves the energy-conversion efficiency. The effect of  $\text{SiN}_x$  layer thickness on the surface reflection property was systematically studied both theoretically and experimentally. The optimized reflectance of theoretical and experimental measurement is 10.50% and 9.39%, respectively. In the stacked  $\text{Al}_2\text{O}_3/\text{SiN}_x$  layers, the results demonstrated that the surface reflection property can be effectively optimized by adding a  $\text{SiN}_x$  layer, which would improve the final photovoltaic characteristic of N-type solar cells with the conversion efficiency as high as 24.85%.

## References

- [1] Macdonald D, Geerligs L J. Recombination activity of interstitial iron and other transition metal point defects in p- and n-type crystalline silicon. *Appl Phys Lett*, 2004, 85: 4061
- [2] Glunz S W, Rein S, Lee J Y, et al. Minority carrier lifetime degradation in boron-doped Czochralski silicon. *J Appl Phys*, 2001, 90: 2397
- [3] Benick J, Hoex B, van de Sanden M C M, et al. High efficiency n-type Si solar cells on Al<sub>2</sub>O<sub>3</sub>-passivated boron emitters. *Appl Phys Lett*, 2008, 92: 253504
- [4] Taguchi M, Tsunomura Y, Inoue H, et al. High-efficiency HIT solar cell on thin (< 100 μm) silicon wafer. 24th European Photovoltaic Solar Energy Conference Hamburg, Germany, 2009: 1690
- [5] Altermatt P P, Plagwitz H, Bock R, et al. The surface recombination velocity at boron-doped emitters: comparison between various passivation techniques. 21st European Photovoltaic Solar Energy Conference Dresden, Germany, 2006: 647
- [6] Hoex B, Heil S B S, Langereis E, et al. Ultralow surface recombination of c-Si substrates passivated by plasma-assisted atomic layer deposited Al<sub>2</sub>O<sub>3</sub>. *Appl Phys Lett*, 2006, 89: 042112
- [7] Hoex B, Schmidt J, Bock R, et al. Excellent passivation of highly doped p-type Si surfaces by the negative-charge-dielectric Al<sub>2</sub>O<sub>3</sub>. *Appl Phys Lett*, 2007, 91: 112107
- [8] Dingemans G, Engelhart P, Seguin R, et al. Stability of Al<sub>2</sub>O<sub>3</sub> and Al<sub>2</sub>O<sub>3</sub>/a-SiN<sub>x</sub>:H stacks for surface passivation of crystalline silicon. *J Appl Phys*, 2009, 106: 114907
- [9] Macleod H A. *Thin-film optical filters*. Bristol: Adam Hilger, 1986
- [10] Bouhafs D, Moussi A, Chikouche A, et al. Design and simulation of antireflection coating systems for optoelectronic devices: application to silicon solar cells. *Solar Energy Materials and Solar Cells*, 1998, 52: 79
- [11] Dingemans G, Kessels W M M. Recent progress in the development and understanding of silicon surface passivation by aluminum oxide for photovoltaics. 25th European Photovoltaic Solar Energy Conference Valencia, Spain, 2010: 1083